

Coexistence of  $\alpha + \alpha + n + n$  and  $\alpha + t + t$  cluster structures in  $^{10}\text{Be}$ N. Itagaki,<sup>1</sup> M. Ito,<sup>2</sup> M. Milin,<sup>3</sup> T. Hashimoto,<sup>4,\*</sup> H. Ishiyama,<sup>4</sup> and H. Miyatake<sup>4</sup><sup>1</sup>*Department of Physics, University of Tokyo, Hongo, 113-0033 Tokyo, Japan*<sup>2</sup>*RIKEN Nishina Center, Wako, 351-0198 Saitama, Japan*<sup>3</sup>*Department of Physics, University of Zagreb, HR-10000 Zagreb, Croatia*<sup>4</sup>*Tokai Radioactive Ion Accelerator Complex, High Energy Accelerator Research Organization (KEK), Tokai, 319-1105 Ibaraki, Japan*

(Received 3 April 2008; revised manuscript received 15 May 2008; published 18 June 2008)

The coexistence of the  $\alpha + \alpha + n + n$  and  $\alpha + t + t$  cluster structures in the excited states of  $^{10}\text{Be}$  has been discussed. In the previous analysis, all the low-lying states of  $^{10}\text{Be}$  were found to be well described by the motion of the two valence neutrons around two  $\alpha$  clusters. However, the  $\alpha + t + t$  cluster structure was found to coexist with the  $\alpha + \alpha + n + n$  structure around  $E_x = 15$  MeV, close to the corresponding threshold. We have introduced a microscopic model to solve the coupling effect between these two configurations. The  $K = 0$  and  $K = 1$  states are generated from the  $\alpha + t + t$  configurations due to the spin coupling of two triton clusters. The present case of  $^{10}\text{Be}$  is one of the few examples in which completely different configurations of triton-type ( $\alpha + t + t$  three-center) and  $\alpha$ -type ( $\alpha + \alpha + n + n$  two-center) clusters coexist in a single nucleus in the same energy region.

DOI: [10.1103/PhysRevC.77.067301](https://doi.org/10.1103/PhysRevC.77.067301)

PACS number(s): 21.60.Gx, 27.20.+n

The importance of  $\alpha$ -like four-body correlations has been extensively investigated for the neutron-rich Be isotopes. The appearance of the cluster rotational band structure in the low-lying states of  $^{10}\text{Be}$  and  $^{12}\text{Be}$  has been reported [1–26], and we have suggested that these states are well described by introducing molecular orbits for the neutrons around the  $\alpha$ - $\alpha$  core [2,18,19]. An anomalously elongated  $\alpha$ - $\alpha$  structure emerges when the valence neutrons occupy the  $\sigma$  orbit along the  $\alpha$ - $\alpha$  axis, which is closely related to the disappearance of the  $N = 8$  magic number in  $^{12}\text{Be}$  [19,27–30].

It has been shown in Fig. 5 of Ref. [18] that the low-lying states of  $^{10}\text{Be}$  are basically well described by molecular orbital model [18,19]; however, corrections are required for the states above the neutron and  $\alpha$  thresholds. This is because strongly correlated subsystems become important (compared with the independent particle motion) in low-density nuclear systems [31–35]. For instance, the calculated third  $0^+$  state in  $^{10}\text{Be}$  around  $E_x = 10$  MeV region (which is not yet experimentally observed) has been found to have an  $\alpha + ^6\text{He}$  structure [22]. In the molecular-orbital picture, each neutron rotates around both  $\alpha$  clusters simultaneously; thus not only the  $\alpha + ^6\text{He}$  configuration but also the  $^5\text{He} + ^5\text{He}$  configuration mixes with the same amplitude (such a picture describes well the first two  $0^+$  states in  $^{10}\text{Be}$ ). On the contrary, in the third  $0^+$  state, the two valence neutrons mainly rotate around the same  $\alpha$  cluster due to the correlations between them; this corresponds to an atomic-orbital structure. Such a coexistence of molecular- and atomic-orbital structures is also recently discussed in the excited states of  $^{12}\text{Be}$  [36].

Furthermore, structures built on various other clusters are expected to appear in the excited states of neutron-rich nuclei around the corresponding threshold energies. In this brief report, we discuss the coexistence of  $\alpha + \alpha + n + n$  and

$\alpha + t + t$  configurations in  $^{10}\text{Be}$ . The excitation energy of the  $\alpha + t + t$  threshold is  $E_x = 19.7$  MeV, which is much higher than the  $\alpha + \alpha + n + n$  threshold ( $E_x = 8.5$  MeV). However, the coexistence of two configurations is expected in the  $E_x \approx 15$  MeV region according to the threshold rule. The existence of the  $^7\text{Li} + t$  cluster configuration has been reported in the recent experiment with the  $^8\text{Li}(d, t)^7\text{Li}$  reaction [37], and since the  $^7\text{Li}$  nucleus is well known to be described as an  $\alpha + t$  cluster structure, the resonance state is considered to have the  $\alpha + t + t$  cluster configuration. The experimental results suggest the possibility of the coexistence of completely different cluster structures of  $\alpha + \alpha + n + n$  and  $\alpha + t + t$  in the excited states of  $^{10}\text{Be}$  [37,38]. This is supported by the fact that a number of states in the  $^{10}\text{Be}$  excitation energy region  $E_x = 9.5$ – $18.0$  MeV is seen by measuring the  $^7\text{Li} + ^7\text{Li}$  reactions at different energies [3,8–10]; the most probable way of producing  $^{10}\text{Be}$  with that entrance channel is a triton transfer to  $^7\text{Li}$  which proves that all the observed states (including the ones identified as molecular) have a nonnegligible overlap with the  $\alpha + t + t$  cluster structure.

The possibility of such a non- $\alpha$  cluster structure has been discussed in neutron-rich nuclei for some time. One recent example is the third  $3/2^-$  state of  $^{11}\text{B}$  at  $E_x = 8.56$  MeV, which is discussed to have the  $\alpha + \alpha + t$  structure from both theoretical and experimental sides [39]. However, the present case of  $^{10}\text{Be}$  is rather different; this is one of the first examples that completely different cluster configurations of triton type and  $\alpha$  type coexist in a single nucleus around the same energy region. A well-known other example is the appearance of  $^4\text{He} + 2n$  and  $t + t$  structures in  $^6\text{He}$  [40,41].

A mechanism for the appearance of cluster structure has been introduced through the so-called Ikeda diagram for  $4N$  nuclei, and the  $\alpha$  cluster is found to be the most important building block of cluster structures [42]. However, due to the weak-binding nature of valence neutrons in the excited states of *neutron-rich nuclei*, various types of the other cluster structures can coexist in the same energy region [36]. In this brief report,

\*Present address: Center for Nuclear Study, University of Tokyo, Hongo, 113-0033 Tokyo, Japan.

we introduce a microscopic model to study the coupling effect between the  $\alpha + \alpha + n + n$  and  $\alpha + t + t$  model spaces and show the appearance of the state(s) that has dominantly the  $\alpha + t + t$  component.

Recently, theoretical investigations for light nuclei based on realistic nucleon-nucleon interactions became feasible [43,44]. However, the most desirable part in these *ab initio* calculations which remains to be performed is the inclusion of many-nucleon correlations, especially the clusterlike correlation. For example, the famous Hoyle state in  $^{12}\text{C}$  ( $0_2^+$ ) and the clusterlike rotational bands in  $^{10}\text{Be}$  and  $^{12}\text{Be}$  related to the intruder orbit ( $1/2^+$ ) cannot be described by the present *ab initio* calculations. Although we use the effective interaction in the present work, description of the cluster states is feasible, so the understanding of the nuclear structure based on such model calculations are in a way complementary to the *ab initio* calculations.

We start with the total wave function, which is fully antisymmetrized and is given by a superposition of the basis states (Slater determinants  $\{\Psi_k\}$ ), with coefficients  $\{c_k\}$ :

$$\Phi = \sum_k c_k P^\pi P_{MK}^J \Psi_k, \quad (1)$$

$$\Psi_k = \mathcal{A}[(\psi_1 \chi_1)(\psi_2 \chi_2) \cdots]_k. \quad (2)$$

Projection onto good parity ( $P^\pi$ ) and angular momentum ( $P_{MK}^J$ ) are performed numerically ( $16^3 = 4096$  mesh points for the Euler angle integral) and the coefficients  $\{c_k\}$  are determined by diagonalizing the Hamiltonian matrix after this projection. Each Slater determinant ( $\Psi_k$ ) consists of  $A$  nucleons, and each nucleon function ( $\psi_i \chi_i$ ,  $i = 1 \sim A$ ) has a Gaussian form [45], i.e.,

$$\psi_i = \left(\frac{2\nu}{\pi}\right)^{\frac{3}{4}} \exp[-\nu(\vec{r} - \vec{z}_i/\sqrt{\nu})^2], \quad (3)$$

where  $\{\chi_i\}$  represent the spin-isospin eigenfunctions. The oscillator parameter is set equal to  $\nu = 1/2b^2$ ,  $b = 1.46$  fm, which is common for all nucleons to exactly remove the center-of-mass kinetic energy. For each Slater determinant ( $\Psi_k$ ), the values of  $\{\vec{z}_i\}$  are randomly generated, and each  $\alpha$  (triton) cluster is expressed by assigning a common  $\vec{z}_i$  value for four (three) nucleons.

To reduce the number of basis states, the selection of Slater determinants is performed after  $J^\pi$  projection. When inclusion of a trial basis state decreases the sum of the energies of the seven lowest states with common  $J^\pi$  ( $0^+$  or  $1^+$ ) by more than 0.05 MeV, the basis state is adopted as in the stochastic variational method (SVM) [46,47] and AMD – superposition of selected snapshots (AMD triple-S) method [48,49]. The selected Slater determinants are projected also to other angular momenta, and the Hamiltonian is diagonalized independently for each  $J^\pi$  state.

The Hamiltonian operator ( $\hat{H}$ ) has the form

$$\hat{H} = \sum_{i=1}^A \hat{t}_i - \hat{T}_{\text{c.m.}} + \sum_{i>j}^A \hat{v}_{ij}, \quad (4)$$

where the two-body interaction ( $\hat{v}_{ij}$ ) includes the central, spin-orbit, and Coulomb parts. As the  $N$ - $N$  interaction, for the

central part, we use the Volkov No.2 effective potential [50]:

$$V(r) = (W - MP^\sigma P^\tau + BP^\sigma - HP^\tau) \times [V_1 \exp(-r^2/c_1^2) + V_2 \exp(-r^2/c_2^2)], \quad (5)$$

where  $c_1 = 1.01$  fm,  $c_2 = 1.8$  fm,  $V_1 = 61.14$  MeV,  $V_2 = -60.65$  MeV,  $W = 1 - M$ , and  $M = 0.60$ . The singlet-even channel of the original Volkov interaction without the Bartlett ( $B$ ) and Heisenberg ( $H$ ) parameters has been known to be too strong, thus  $B = H = 0.125$  is introduced. For the spin-orbit term, we introduce the G3RS potential [51]:

$$V_{ls} = V_0(e^{-d_1 r^2} - e^{-d_2 r^2})P(^3O)\vec{L} \cdot \vec{S}, \quad (6)$$

where  $d_1 = 5.0 \text{ fm}^{-2}$ ,  $d_2 = 2.778 \text{ fm}^{-2}$ ,  $V_0 = 2000$  MeV, and  $P(^3O)$  is a projection operator onto a triplet odd state. The operator  $\vec{L}$  stands for the relative angular momentum, and  $\vec{S}$  is the spin ( $\vec{S}_1 + \vec{S}_2$ ). All the parameters of this interaction are the same as those used in our previous work [18–20], and they were determined from the  $\alpha + n$  and  $\alpha + \alpha$  scattering phase shifts [52], which are shown to describe well the low-lying states of  $^{10}\text{Be}$ .

With such a model, the calculated  $^{10}\text{Be}$  energy levels (positive parity) assuming the equilateral triangular shape of the  $\alpha + t + t$  configurations are shown in Fig. 1 (the basis states with various relative distances of this shape are superposed). Since the triton clusters have  $S = 1/2$ , the system can have total spin of both  $S = 0$  and  $S = 1$ . Because of this spin structure,  $K = 0(S_z = 0)$  and  $K = 1(S_z = 1)$  states of  $^{10}\text{Be}$  are generated from the  $\alpha + t + t$  configurations. The left-hand side of the figure ( $0^+, 2^+, 4^+$ ) shows the  $K = 0$  states, and the right-hand side ( $1^+, 2^+, 3^+, 4^+$ ) shows the  $K = 1$  states. The horizontal lines at  $-55.1$  and  $-41.3$  MeV show the threshold energies of  $\alpha + \alpha + n + n$  and  $\alpha + t + t$ , respectively. In contrast to the Hoyle state in  $^{12}\text{C}$ , it can be seen that the states appear slightly below the  $\alpha + t + t$  threshold. This is due to the attractive interaction among the clusters; although  $\alpha + \alpha$  ( $^8\text{Be}$ ) does not have a bound state,  $\alpha + t$  ( $^7\text{Li}$ ) has a bound state (even two). The energy intervals of the levels in each  $K = 0$  and  $K = 1$  category deviate from the  $J(J + 1)$  rule, and this is due to the contribution of the spin-orbit interaction. For instance, although the energy interval between the  $1^+$  and  $2^+$  states with  $K = 1$  is only 140 keV, this splitting

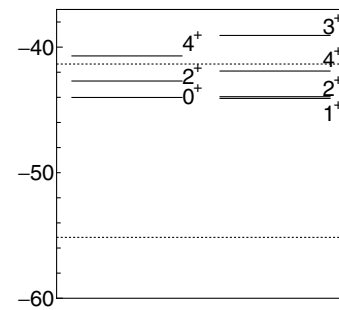


FIG. 1. Energy levels of  $^{10}\text{Be}$  (positive parity) calculated assuming the equilateral triangular shape of the  $\alpha + t + t$  configurations. The left-hand side shows the  $K = 0$  case; right-hand side,  $K = 1$ . The horizontal lines at  $-55.1$  and  $-41.3$  MeV show the thresholds of  $\alpha + \alpha + n + n$  and  $\alpha + t + t$ , respectively.

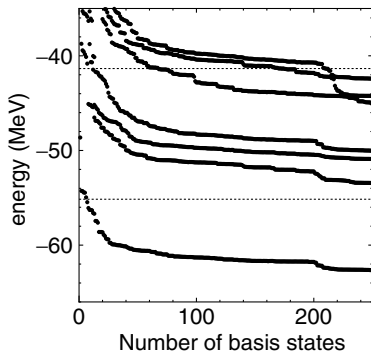


FIG. 2. Energy convergence of the seven lowest  $0^+$  states of  $^{10}\text{Be}$  as a function of the number of Slater determinants introduced.

increases to 1 MeV when the spin-orbit interaction is switched off. Although they are not shown in this figure, the negative parity states are also generated from these basis states above the threshold.

In the next step, the model is extended from the equilateral triangular shape to various  $\alpha + t + t$  configurations. The coupling condition with the different cluster configuration of  $\alpha + \alpha + n + n$  is also imposed. Figure 2 shows the results for  $0^+$  ( $S_z = 0$  for protons and neutrons) states, where the energy convergence of the seven lowest  $0^+$  states of  $^{10}\text{Be}$  is given as a function of the number of basis states. The basis states with the  $\alpha + \alpha + n + n$  configurations are used from 1 to 200 on the horizontal axis (it has been discussed in Ref. [19] that basis states with  $S_z = 1$  for the two neutrons are required for quantitative description of the second  $0^+$  state; however, this configuration is omitted for simplicity) and after obtaining the convergence, the basis states with  $\alpha + t + t$  configurations are superposed (from 201 to 250). It is clearly seen that the energy of one of the  $0^+$  states drastically decreases after the model starts incorporating the  $\alpha + t + t$  configurations in the model space (beyond 200), and finally, the energy of this state converges at  $-45.0$  MeV as the fifth  $0^+$  state. Therefore, the fifth  $0^+$  state of  $^{10}\text{Be}$  is considered to have a large contribution from the  $\alpha + t + t$  configurations, and the state is stable even after taking into account the coupling with the  $\alpha + \alpha + n + n$  configurations. The converged energy of this state is slightly lower than that of the  $0^+$  state in Fig. 1 (obtained assuming the equilateral triangular shape) by about 0.5 MeV because of the many additional configurations used; but basically we can confirm that the deviation from the result of Fig. 1 is small. The calculated rms radius (proton part) of the fifth  $0^+$  state is 2.75 fm, which is smaller than the value for the second  $0^+$  state (2.95 fm, well-known state to have large  $\alpha$ - $\alpha$  clustering enhanced by the valence neutrons in the  $\sigma$  orbitals [18]); however, it is significantly larger than the one for the ground state (2.43 fm). The obtained basis states can be projected to other  $J^\pi$  states. Three positive-parity band structures appear in the low-lying energy region, similar to that in Ref. [18]. The ground  $0^+$  and the  $2_1^+$  state calculated at  $E_x = 3.4$  MeV mainly have the  $K = 0$  component (ground band), and the  $2_2^+$  state at  $E_x = 5.6$  MeV and the  $3_1^+$  state at  $E_x = 8.9$  MeV have mainly the  $K = 2$  component ( $K = 2$  band). The  $4_1^+$  state at  $E_x = 10.5$  MeV has both  $K = 0$  and  $K = 2$  components. The

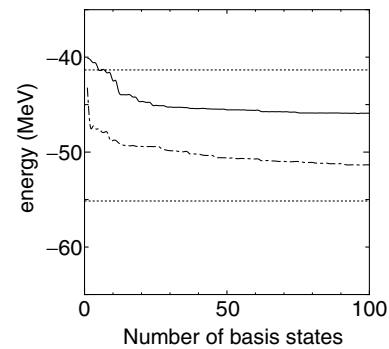


FIG. 3. Energy convergence of the  $1^+$  ( $K = 1$ ) states of  $^{10}\text{Be}$  as a function of the number of Slater determinants introduced. The solid and dash-dotted lines are the cases of  $\alpha + t + t$  and  $\alpha + \alpha + n + n$  configurations, respectively.

second  $0^+$  state (calculated at  $E_x = 9.0$  MeV) is a band head of the cluster rotational band ( $2_3^+$  at  $E_x = 10.3$  MeV and  $4_2^+$  at  $E_x = 12.9$  MeV belong to this band), which has a much larger moment of inertia than that of the ground band.

For the  $K = 1$  states, the energy convergence of the  $1^+$  states is shown in Fig. 3 as a function of the number of basis states. Contrary to the  $0^+$  case, only two  $1^+$  states appear in this energy region. The solid line is calculated by superposing various  $\alpha + t + t$  configurations, where spin orientation of two triton clusters are taken to be parallel ( $S_z = 1$ ), and the intrinsic angular momentum of  $K = 1$  is generated from the spin part of the protons in the tritons. The converged energy of  $-45.6$  MeV is below the  $\alpha + t + t$  threshold because of the interaction among the clusters, and the energy is slightly lower than the case of the equilateral triangular shape in Fig. 1 ( $-44.1$  MeV). For the  $\alpha + \alpha + n + n$  model space, it has been shown that one  $1^+$  state appears around the  $E_x = 10$  MeV region [18], when the spin orientation of the two valence neutrons are taken to be parallel. Therefore, in  $\alpha + \alpha + n + n$  model space, the intrinsic angular momentum of  $K = 1$  is generated from the spin part of the valence neutrons, and the dash-dotted line shows the energy convergence of this configuration. Since the spin structures of these two  $1^+$  states are completely different, the overlap and coupling effect between these states is small. As a result, the  $K^\pi = 1^+$  states with the  $\alpha + t + t$  configurations appear at almost the same energy as the  $K^\pi = 0^+$  states slightly below the  $\alpha + t + t$  threshold, due to the small energy difference between the spin-singlet and spin-triplet configurations of two tritons.

Experimentally, the resonance state with the  $\alpha + t + t$  configuration has been reported to appear slightly above the corresponding threshold energy [37,38]. There is a possibility that the state observed in the experiment corresponds to a calculated state (with rather large  $J$  of 3 or 4) or a small  $J$  state of excited band including the negative parity bands. To calculate the excited rotational band structure above the threshold, it would be necessary to impose the condition of the resonance state to eliminate the continuum components. Nevertheless, the present case of  $^{10}\text{Be}$  is one of the first examples that completely different configurations of triton-type ( $\alpha + t + t$  three-center) and  $\alpha$ -type ( $\alpha + \alpha + n + n$

two-center) clusters coexist in a single nucleus around the same energy region.

One of the authors (N.I.) would like to thank the JSPS core-to-core program.

- 
- [1] A. A. Korscheninnikov *et al.*, Phys. Lett. **B343**, 53 (1995).  
 [2] W. von Oertzen, Z. Phys. A **354**, 37 (1996); **357**, 355 (1997).  
 [3] N. Soić *et al.*, Europhys. Lett. **34**, 7 (1996).  
 [4] M. Milin *et al.*, Nucl. Phys. **A753**, 263 (2005).  
 [5] M. Freer *et al.*, Phys. Rev. Lett. **82**, 1383 (1999).  
 [6] M. Freer *et al.*, Phys. Rev. C **63**, 034301 (2001).  
 [7] M. Freer *et al.*, Phys. Rev. Lett. **96**, 042501 (2006).  
 [8] N. R. Fletcher, D. D. Caussyn, F. Marechal, M. Curtis, and J. A. Liendo, Phys. Rev. C **68**, 024316 (2003).  
 [9] N. Curtis *et al.*, Phys. Rev. C **64**, 044604 (2001).  
 [10] N. Curtis *et al.*, Phys. Rev. C **70**, 014305 (2004).  
 [11] N. Curtis *et al.*, Phys. Rev. C **73**, 057301 (2006).  
 [12] N. I. Ashwood *et al.*, Phys. Rev. C **68**, 017603 (2003).  
 [13] N. I. Ashwood *et al.*, Phys. Lett. **B580**, 129 (2004).  
 [14] N. I. Ashwood *et al.*, Phys. Rev. C **72**, 024314 (2005).  
 [15] H. G. Bohlen *et al.*, Phys. Rev. C **75**, 054604 (2007).  
 [16] Y. Kanada-En'yo, H. Horiuchi, and A. Doté, Phys. Rev. C **60**, 064304 (1999).  
 [17] Y. Kanada-En'yo and H. Horiuchi, Phys. Rev. C **68**, 014319 (2003).  
 [18] N. Itagaki and S. Okabe, Phys. Rev. C **61**, 044306 (2000).  
 [19] N. Itagaki, S. Okabe, and K. Ikeda, Phys. Rev. C **62**, 034301 (2000).  
 [20] N. Itagaki, S. Hirose, T. Otsuka, S. Okabe, and K. Ikeda, Phys. Rev. C **65**, 044302 (2002).  
 [21] M. Ito, K. Kato, and K. Ikeda, Phys. Lett. **B588**, 43 (2004).  
 [22] Makoto Ito, Phys. Lett. **B636**, 293 (2006).  
 [23] Y. Ogawa, K. Arai, Y. Suzuki, and K. Varga, Nucl. Phys. **A673**, 122 (2000).  
 [24] Koji Arai, Phys. Rev. C **69**, 014309 (2004).  
 [25] Jim Al-Khalili and Koji Arai, Phys. Rev. C **74**, 034312 (2006).  
 [26] P. Descouvemont, Nucl. Phys. **A699**, 463 (2002).  
 [27] H. Iwasaki *et al.*, Phys. Lett. **B481**, 7 (2000).  
 [28] H. Iwasaki *et al.*, Phys. Lett. **B491**, 8 (2000).  
 [29] A. Navin *et al.*, Phys. Rev. Lett. **85**, 266 (2000).  
 [30] S. Shimoura *et al.*, Phys. Lett. **B560**, 31 (2003).  
 [31] G. F. Bertsch and H. Esbensen, Ann. Phys. (NY) **209**, 327 (1991).  
 [32] Shigeyoshi Aoyama, Shigeo Mukai, Kiyoshi Katō, and Kiyomi Ikeda, Prog. Theor. Phys. **93**, 99 (1995).  
 [33] Masayuki Matsuo, Kazuhito Mizuyama, and Yasuyoshi Serizawa, Phys. Rev. C **71**, 064326 (2005).  
 [34] K. Hagino and H. Sagawa, Phys. Rev. C **72**, 044321 (2005).  
 [35] T. Nakamura *et al.*, Phys. Rev. Lett. **96**, 252502 (2006).  
 [36] M. Ito, N. Itagaki, H. Sakurai, and K. Ikeda, Phys. Rev. Lett. **100**, 182502 (2008).  
 [37] T. Hashimoto *et al.*, AIP Conf. Proc. **1016**, 313 (2008).  
 [38] R. O. Nelson and A. Michaudon, Nucl. Sci. Eng. **140**, 195 (2002).  
 [39] T. Kawabata *et al.*, Phys. Lett. **B646**, 6 (2007).  
 [40] A. Csótó, Phys. Rev. C **48**, 165 (1993).  
 [41] T. Yamagata *et al.*, Phys. Rev. C **71**, 064316 (2005).  
 [42] K. Ikeda, N. Takigawa, and H. Horiuchi, Prog. Theor. Phys. Suppl. Extra number, 464 (1968).  
 [43] R. B. Wiringa, Steven C. Pieper, J. Carlson, and V. R. Pandharipande, Phys. Rev. C **62**, 014001 (2000).  
 [44] D. C. Zheng, B. R. Barrett, L. Jaqua, J. P. Vary, and R. J. McCarthy, Phys. Rev. C **48**, 1083 (1993).  
 [45] D. M. Brink, in *Proceedings of the International School of Physics "Enrico Fermi" Course 36*, edited by C. Bloch (Academic, New York, 1966), p. 247.  
 [46] V. I. Kukulin and V. M. Krasnopol'sky, J. Phys. A **10**, 33 (1977).  
 [47] K. Varga, Y. Suzuki, and Y. Ohbayasi, Phys. Rev. C **50**, 189 (1994).  
 [48] N. Itagaki, A. Kobayakawa, and S. Aoyama, Phys. Rev. C **68**, 054302 (2003).  
 [49] N. Itagaki, S. Aoyama, S. Okabe, and K. Ikeda, Phys. Rev. C **70**, 054307 (2004).  
 [50] A. B. Volkov, Nucl. Phys. **74**, 33 (1965).  
 [51] R. Tamagaki, Prog. Theor. Phys. **39**, 91 (1968); **62**, 1018 (1979).  
 [52] S. Okabe and Y. Abe, Prog. Theor. Phys. **61**, 1049 (1979).